Fractal nature of multiple shear bands in severely deformed metallic glass

B. A. Sun and W. H. Wang[a)]
Institute of Physics, Chinese Academy of Sciences, Beijing 100190, People's Republic of China

(Received 5 March 2011; accepted 27 April 2011; published online 16 May 2011)

We present an analysis of fractal geometry of extensive and complex shear band patterns in a severely deformed metallic glass. We show that the shear band patterns have fractal characteristics, and the fractal dimensions are determined by the stress noise induced by the interaction between shear bands. A theoretical model of the spatial evolution of multiple shear bands is proposed in which the collective shear bands slide is considered as a stochastic process far from thermodynamic equilibrium. © *2011 American Institute of Physics*. [doi:10.1063/1.3592249]

At ambient temperature plastic deformation of most metallic glasses (MGs) is inhomogeneous with plastic strains confined to thin shear bands and serrated flow in stress-strain curves.[1–7] For a few ductile MGs (Ref. 8 and 9) or MG samples with low aspect ratio,[10] multiple shear bands are observed. The network pattern formed by the branching and multiplication of shear bands can effectively dissipate the plastic energy and alleviate stress concentration, thus, leading to large compressive plasticity. The spatial evolution of these multiple shear bands as well as the underlying physical mechanism, however, is still poorly understood.

Most analyses on shear bands of MGs are based on the mean-field free volume[11] or shear transformation zone (STZ) theory.[1] The temporal or spatial correlation between shear bands is often neglected. But in some cases, shear band patterns are complex and appear on various scales with the feature of randomness and heterogeneity. A few studies have also shown the importance of shear bands interaction on the plasticity of MGs.[12,13] In this letter, we present a fractal analysis of the complex multiple shear bands patterns in a severely deformed MG. The result as well as its implications for the plastic deformation mechanism of MGs is interpreted in terms of a proposed stochastic model of spatial evolution of multiple shear bands.

Cubic plastic $Zr_{64.13}Cu_{15.75}Ni_{10.12}Al_{10}$ MG samples[9] with a size of $1.5\times1.5\times1.5$ mm were used in the compression tests, as it was reported that large plastic strains can be obtained for specimens with aspect ratio lower than 1.[10] Figure 1 shows a typical stress-strain curve with compressive strain up to 40% for the MG. Obvious serrated flow can be seen in the curve. The statistical analysis on serrations[13] in this curve give a power distribution $D(s)=s^{-1.40}$, where $D(s)$ is the probability density of the serration magnitude s, indicating shear band interaction may play a role in the complex, scale-free shear process. The stress curve with a clear upward drift with strains cannot be ascribed to strain-hardening behavior of MG, as reflected from the true stress-strain curve with almost constant flow stress for shear bands in the plastic regime.[14]

Figure 2(a) shows a typical scanning electron micrograph (SEM) of multiple shear bands pattern as observed from the side surface of sample at plastic strain of 40%. The pattern is highly heterogeneous in the shear band density distribution and seems appear in various scale (see the magnified region in Fig. 2(b) with much finer shear bands). Clearly, the average shear band spacing cannot be well defined. The shear band patterns at other large plastic strains also show similar characters. The fractal analysis[15] was then used to characterize these complex patterns. The micrographs can be regarded as consisting of the shear band patterns and the undeformed matrix cells surrounded by shear bands. According to their different contrasts, we first digitize the images into binary maps ("white" for shear bands and "black" for matrix cells). The box-counting method is then applied to estimate the fractal dimension. For grids of square boxes with edge length Δx, the number $N(\Delta x)$ of boxes covering at least one pixel of a shear band has the relation of $N(\Delta x)\sim\Delta x^{-D_B}$, where D_B is typically a noninteger number called "box-counting" dimension for a fractal pattern. The double-logarithmic plots of $N(\Delta x)$ versus Δx corresponding to the shear band patterns at strain of 40% are shown in Fig. 3(a). A clear linear scaling regime extended more than one order of magnitude of Δx with the box dimension $D_B=1.53\pm0.02$ can be seen in the plot, which is the typical feature of a fractal. Deviations from the linear region at both ends are also observed, often arising from finite size effect of actual fractal objects.[15] In our case, the slight deviation at the beginning of the linear regime may be due to finite thickness of shear bands. At large Δx, the relation $N(\Delta x)\sim\Delta x^{-2}$

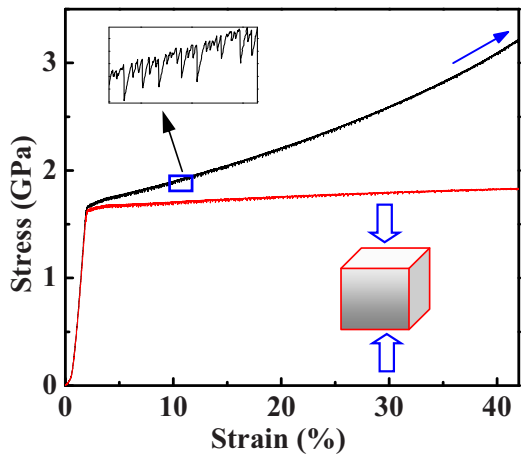

FIG. 1. (Color online) The compressive stress-strain curves of the cubic MG sample at the strain rate 5×10^{-4} s^{-1}: the black is the engineering stress-strain curve and the red is the true stress-strain curve. Obvious serrations can be observed from the magnified part of the stress curve in the plastic regime.

a)Author to whom correspondence should be addressed. Electronic mail: whw@iphy.ac.cn.

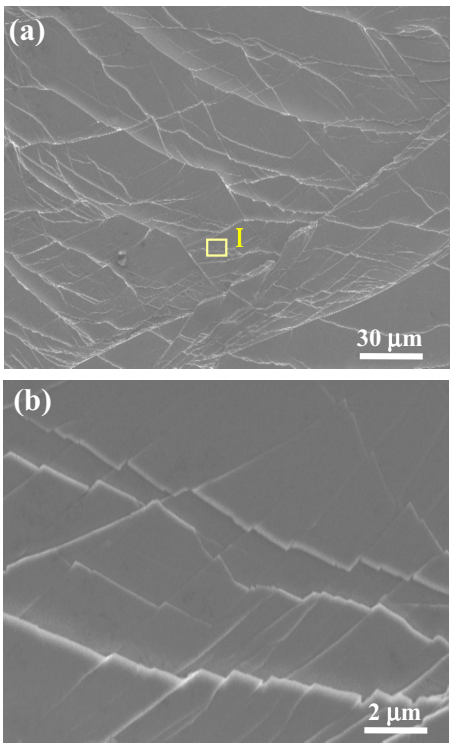

FIG. 2. (Color online) SEM micrographs of multiple shear band patterns observed from the side surface of the MG (a) patterns at plastic strain of 40% and (b) the magnified shear bands of the region I in (a).

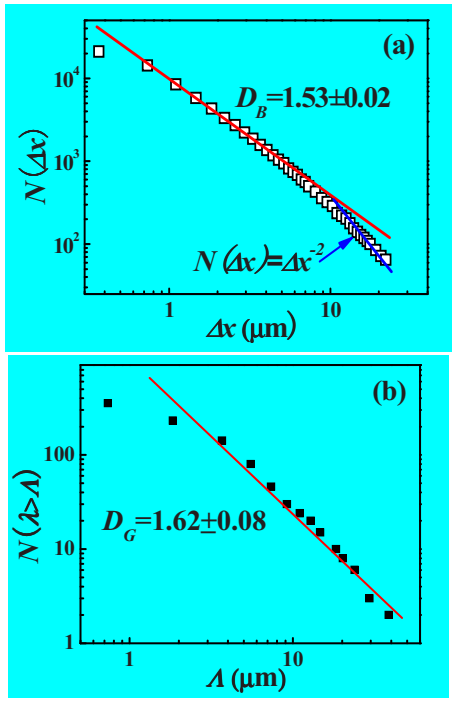

FIG. 3. (Color online) Fractal analysis of shear band patterns in Fig. 2(a): (a) The $N(\Delta x) \sim \Delta x$ relation obtained by counting box method. (b) The cumulative frequency distribution $N(\lambda > \Lambda)$ of cell size surrounded by shear bands.

holds, indicating after a critical edge length of box, the analyzed area is covered completely. The fractal nature of shear band pattern is corroborated by analyzing the size distribution of matrix cells surrounded by shear bands. For a hole fractal in two dimensions, the cumulative frequency distribution $N(\lambda > \Lambda)$ of cells with linear sizes larger than Λ has the relation of $N(\lambda > \Lambda) = C\Lambda^{-D_G}$, where D_G is called the "gap dimension."[16] Here, we define the linear size λ of a cell as $\lambda = \sqrt{S}$ with S being the area of cell. The prefactor C depends on the cell shape, fractal dimension D_G and the analyzed area A and reads $C = [A(2-D_G)/D_G]^{D_G/2}$ for square cells by assuming that the scaling regime extends up to the cell size where the cumulative frequency distribution falls below 1. The cumulative cell size distribution for the shear band patterns at plastic strain of 40% are depicted in Fig. 3(b). A linear scaling regime over more than one order of magnitude of cell size is also found. The gap dimension D_G and log C determined by fitting the experimental data are 1.62 ± 0.08 and 3.02, respectively. The value of D_G coincides with D_B, suggesting that the roughness of shear bands does not affect the fractal dimension. We also note that the fitting values of C, D_G, and the analyzed area A $(3.9 \times 10^4\ \mu m^2)$ well satisfy the relation $C = [A(2-D_G)/D_G]^{D_G/2}$, which strongly suggests that the scaling is genuine and only delimited by finite size effects. The shear band patterns at other large plastic strains are also analyzed by the fractal method yielding similar results (for example, at plastic strain of 60%, $D_B = 1.63 \pm 0.02$, and $D_G = 1.58 \pm 0.07$). The formation of fractals can be interpreted as the intersections between different orders of shear bands with different directions and various spacing, as illustrated in Fig. 4(a). Despite the real shear band patterns appear more randomly and heterogeneously, the schematic pattern shown in Fig. 4 indeed resemble that of Fig. 2. It should be noted that the multiple shear band patterns in the present analysis is induced by geometrical constraints of samples, thus, the fractal geometry cannot be universally applicable to shear band patterns generated under other load conditions.

To theoretically understand above results, we propose a stochastic model for the spatial evolution of shear bands. The

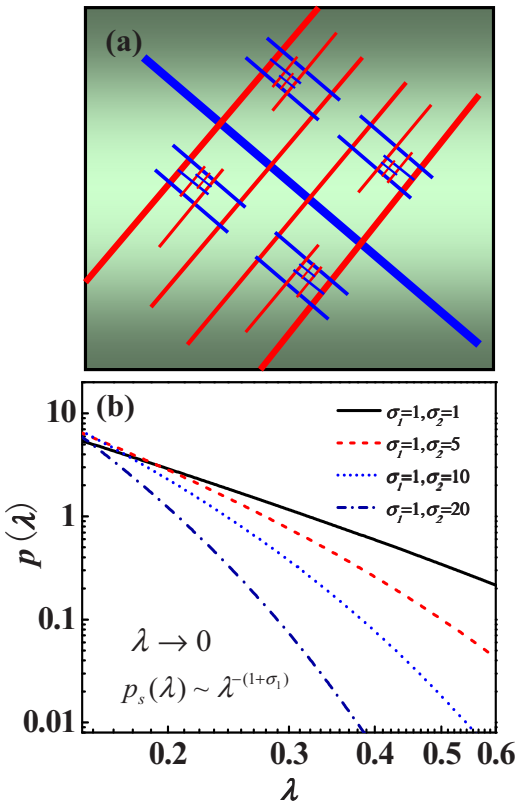

FIG. 4. (Color online) (a) Schematic diagram of the fractal pattern for shear bands. (b) The calculated density distribution $p(\lambda)$ of shear band spacing λ for different values of σ_1 and σ_2.

fractal geometry suggests that the evolution of multiple shear bands is a process of far from thermodynamic equilibrium and interaction between shear bands should be considered. According to the free volume or STZ theory,[1,11] shear bands in the absent of interaction can operate under a steady state stress τ_s which is regarded as a smooth function in space and time. Here, we consider that the transient shear band interaction can induce fluctuating internal stress τ_{int} on operating shear bands. As τ_{int} varied much rapidly than τ_s, we assume that τ_s is a constant in the time scale of the transient interaction, thus τ_{int} can be regarded as stress noises exerted on τ_s. For the collective operating shear bands, the effective stress τ_{eff} is $\tau_{\text{eff}}=\tau_s+\tau_{\text{int}}$. It must be pointed out that the fluctuating stress cannot solely be attributed to the shear band interaction. Recent studies show that the flow serrations may also arise from the stick-slip motion of a single shear band.[2,3] As our goal is mainly to give a possible theory for the formation of fractal pattern of shear bands, a full stochastic model by incorporating the stick-slip dynamics of shear bands is obviously beyond the scope of this study.

For the inhomogeneous deformation process in MGs, the local shear strain rate $\dot{\gamma}$ is expressed as[1] $\dot{\gamma}=\dot{\gamma}_0 \exp(-\Delta G - \tau_{\text{eff}} V_{\text{ap}}/k_B T)$, where $\dot{\gamma}_0$ is a characteristic shear strain rate, ΔG is the total energy barrier, and V_{ap} is the activation volume. According to this equation, the fluctuation of stress gives rise to spatiotemporal variation in $\dot{\gamma}$ and thus heterogeneity in the distribution of shear band patterns. Instead of treating microscopic details (which is impossible in analytical modeling), we proceed by considering the mesoscopic properties of the internal stress τ_{int} from its noise character. The fluctuation amplitude of τ_{int} is derived by assuming the deformation is in the quasistatic stress equilibrium and using Furutsu–Novikov theorem with an analogy of shear bands to dislocations:[17] $\langle \tau_{\text{int}} \rangle = S\langle \delta\dot{\gamma}^2 \rangle / \langle \dot{\gamma} \rangle$, where $\langle \cdot \rangle$ denotes the temporal average effect over a sufficiently long interval of time during the operation of shear bands, $S=\partial \ln\langle \tau_{\text{eff}} \rangle / \partial \ln\langle \dot{\gamma} \rangle$ is the strain rate sensitivity representing the dynamic response function to the average imposed $\dot{\gamma}$. This suggests that the fluctuating internal stress cannot be viewed as purely white noises. Generally, the τ_{int} is a function of γ, $\dot{\gamma}$, and stochastic noise δw with $\langle \delta w(t)\delta w(t') = 2\delta(t) \rangle : \tau_{\text{int}} = \tau_{\text{int}}(\gamma, \dot{\gamma}, \delta w)$. The values of strain rate sensitivity is usually small for MGs,[3,18] hence, we neglect the strain rate dependence of τ_{int} and assume τ_{int} is only the linear function of γ and δw: $\tau_{\text{int}} = A\gamma + B\delta w$, where A and B are the weighting factors of the deterministic and stochastic parts of the τ_{int}, respectively. The linear dependence of τ_{int} on γ can be understood from the fact that more shear bands will be induced as the plastic strain increases, yielding higher τ_{int}. Taking τ_{int} into the local strain rate equation, using Taylor expansion and keeping the linear terms, we obtain the temporal evolution of the local plastic strain γ

$$\dot{\gamma} = R + (RAV_{\text{ap}}/k_B T)\gamma + (RBV_{\text{ap}}/k_B T)\gamma\delta w, \tag{1}$$

where $R=\dot{\gamma}_0 \exp(-\Delta G - \tau_s V_{\text{ap}}/k_B T)$ is the constant strain rate produced by the steady state stress. Equation (1) is a typical Langevin equation. The steady-state probability distribution $p_s(\gamma)$ of γ is obtained by solving the Fokker –Planke equation corresponding to Eq. (1). Using the Stratonovich calculus, $p_s(\gamma)$ reads

$$p_s(\gamma) = N\gamma^{-(1-\sigma_1)} \exp(-\sigma_2/\gamma), \tag{2}$$

where σ_1 and σ_2 are defined as $\sigma_1 = Ak_B T/(RV_{\text{ap}}B^2)$, $\sigma_2 = k_B^2 T^2/(RV_{\text{ap}}^2 B^2)$, and N is a normalization constant. The statistical information relevant to shear band patterns can be obtained from Eq. (2) if the relation between the plastic strain and shear bands is known. Bei *et al.*[10] found that the average spacing of shear bands decrease linearly with the overall plastic strain γ: $\lambda \sim \gamma^{-1}$. Assuming that this relation only holds for the local area on the surface of the sample, Eq. (2) is then transformed into the shear band spacing distribution by change in variables $p_s(\lambda)d\lambda = p_s(\gamma)d\gamma$

$$p_s(\lambda) \sim \lambda^{-(1+\sigma_1)} \exp(-\sigma_2\lambda). \tag{3}$$

The probability distributions $p_s(\lambda)$ decreases monotonically with λ for various values of σ_1, σ_2, as illustrated in Fig. 4(b). When $\lambda < \lambda_{\max} = 1/\sigma_2$, the exponential term becomes trivial and $p_s(\lambda)$ diverges to $\lambda^{-(1+\sigma_1)}$ as λ goes to zero. The hyperbolic distribution reflects the fact that shear bands organize on various scales up to the maximum shear band spacing $\lambda_{\max} = 1/\sigma_2$. In heavily deformed MGs, the density of shear bands is very high and the corresponding λ is usually very small. Thus, the corresponding cumulative cell size distribution function $P(\lambda > \Lambda)$ behaves as $P(\lambda > \Lambda) \sim \Lambda^{-\sigma_1}$. This is consistent with the form of the above experimental cumulative cell size distribution of $N(\lambda > \Lambda) = C\Lambda^{-D_G}$. So the fractal dimension is in fact equal to the parameter σ_1 which is determined by the weighting factors A and B. Therefore, our stochastic model gives a theoretical explanation for the formation of fractal patterns of multiple shear bands during the deformation of MGs.

The financial support is from the NSF of China (Grant Nos. 50731008 and 50921091) and MOST 973 of China (Grant No. 2007CB613904 and 2010CB731603).

[1] A. S. Argon, Acta Metall. **27**, 47 (1979).
[2] R. Maaß, D. Klaumünzer, and J. F. Löffler, Acta Mater. **59**, 3205 (2011).
[3] S. X. Song, H. Bei, J. Wadsworth, and T. G. Nieh, Intermetallics **16**, 813 (2008).
[4] W. J. Wright, M. W. Samale, T. C. Hufnagel, M. M. LeBlanc, and J. N. Florando, Acta Mater. **57**, 4639 (2009).
[5] F. H. Dalla Torre, D. Klaumünzer, R. Maaß, and J. F. Löffler, Acta Mater. **58**, 3742 (2010).
[6] D. Klaumünzer, R. Maaß, F. H. D. Torre, and J. F. Löffler, Appl. Phys. Lett. **96**, 061901 (2010).
[7] M. F. Ashby and A. L. Greer, Scr. Mater. **54**, 321 (2006).
[8] J. Schroers and W. L. Johnson, Phys. Rev. Lett. **93**, 255506 (2004).
[9] Y. H. Liu, G. Wang, R. J. Wang, D. Q. Zhao, M. X. Pan, and W. H. Wang, Science **315**, 1385 (2007).
[10] H. Bei, S. Xie, and E. P. George, Phys. Rev. Lett. **96**, 105503 (2006).
[11] F. Spaepen, Acta Metall. **25**, 407 (1977).
[12] J. Zhang, P. Aimedieu, F. Hild, S. Roux, and T. Zhang, Scr. Mater. **61**, 1145 (2009).
[13] B. A. Sun, H. B. Yu, W. Jiao, H. Y. Bai, D. Q. Zhao, and W. H. Wang, Phys. Rev. Lett. **105**, 035501 (2010).
[14] Z. Han, H. Yang, W. F. Wu, and Y. Li, Appl. Phys. Lett. **93**, 231912 (2008).
[15] T. Vicsek, *Fractal Growth Phenomena* (World Scientific, Singapore, 1992).
[16] P. Hähner, K. Bay, and M. Zaiser, Phys. Rev. Lett. **81**, 2470 (1998).
[17] P. Hähner, Acta Mater. **44**, 2345 (1996).
[18] D. Pan, A. Inoue, T. Sakurai, and M. W. Chen, Proc. Natl. Acad. Sci. U.S.A. **105**, 14769 (2008).